Journal of Chemical Engineering, IEB
Vol. ChE. 27, No. 1, June 2012

Drying Induced Phase Separation

Raj Kumar Arya

Department of Chemical Engineering, Jaypee University of Engineering and Technology, Guna,
A.B. Road, Raghogarh, Guna - 473226, M.P., India

Abstract

Polymeric Membrane can be produced by several methods. This paper deals computational study to prepare polymeric membrane using drying. Asymmetric and symmetric membranes can be prepared by changing the drying parameters like air flow rates, drying temperatures, and coating compositions.

Keywords *Polymeric Coatings, Asymmetric Membranes, Symmetric Membranes, Drying, Phase Separation*

1. Introduction

Polymeric membranes are used in large scale in membrane filtration and other separation techniques. There are two types of membranes asymmetric and symmetric. Each of them has its own advantages. These membranes are manufactured by phase separation processes of homogenous polymer solutions. During phase separation, macrovoids are formed that are useful in drug delivery systems, ultra-filtration, composite membrane supports, bioreactors, screen printing media and breathable fabrics (Penky et al., 2003). Macrovoids are the pores of having size distribution of 10-50μm. Phase inversion can be achieved by wet casting process, dry casting process, vapor induced phase separation, and thermally induced phase separation (Altinkaya and Ozbas, 2004 and Matsuyama et al., 2000).

In wet cast process, polymer casting solution is immersed in the nonsolvent bath which results formation of porous membranes due the solvent loss and counter diffusion of nonsolvent into the casting solution (Shojaie et al., 1994).
Thermally induced phase separation process begins by dissolving the polymer into the diluent at elevated temperature. After that the solution is to be casted in desired shape and subjected in cooling to induce phase separation. By solvent exchange process diluent is extracted and the evaporation of extractant yields a microporous structure (Matsuyama et al., 2004).

Dry cast process is one of the process by which thermodynamic state of polymer solution can be altered to achieve the phase inversion. It is characterized by evaporation of nonsolvent and solvent from initially homogeneous single phase solution (Shojaie et al., 1994 and Young et al., 2002). Due to external effects homogenous polymer solution becomes thermodynamically unstable initially (Altinkaya and Ozbas, 2004) and two phase solution is formed due to evaporation. Hence phase separates into polymer lean and polymer rich phases. On solidification polymer rich phase precipitated to form solid matrix that envelops the polymer lean phase that is rich in solvent and nonsolvent fill the pores. This process avoids the complication associated with the use of coagulation baths as in wet cast process. Polymer concentration is increased to reduce the solvation character of polymer solvent as the solvent is evaporated from the solution (Young et al., 2002). Evaporation step significantly influences the final membrane morphology in dry and wet cast phase inversion process.

If the drying rate is high and coating thickness is small, top surface becomes dense in polymer due to high rate of solvent and nonsolvent evaporation which is called trapping skinning. Once the skin formation takes place, the nonsolvent penetrates the skin at the weak spots and it initiates the macrovoids (Shojaie et al., 1994). Below the skin layer liquid-liquid phase separation takes place (Koenhen et al., 1977). Liquid –liquid phase separation takes place when a homogeneous solution becomes thermodynamically unstable due to introduction of a non solvent. Original solution decreases its free energy of mixing by splitting up into two liquid phases of different composition (Broens et al., 1980). Liquid-liquid demixing is caused either by nucleation and growth or spinodal decomposition. Nucleation growth mechanism occurs in metastable region between spinodal and bimodal however spinodal decomposition occurs in the unstable region inside the spinodal curve (Matsuyama et al., 2000).

Structure is evolved by spinodal decomposition mechanism if composition passes through the critical point and phase separation occurs in the unstable region. If the composition passes slowly in the metastable region, phase separation occurs in nucleation growth region. This followed by the growth of macrovoids because of diffusion of solvent and nonsolvent from the surrounding polymer solution and precipitation bath. During dry casting process and precipitation in wet casting process macrovoids are formed.

* Corresponding Author: Dr. Raj Kumar Arya
Email: raj.arya@juet.ac.in , Fax: +91-7544-267011,

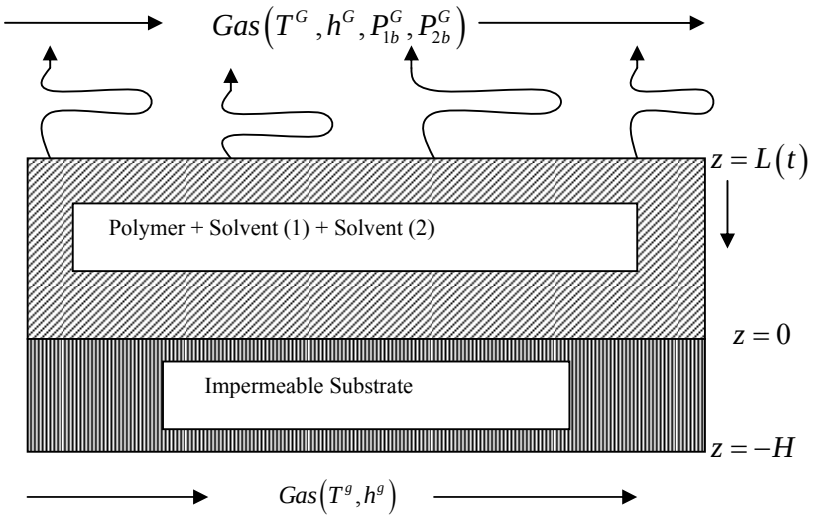

Fig.1. Schematic of a drying coating

Macrovoids formation can be eliminated by decreasing the rate of evaporation. Macrovoids appear to occur in the systems that begin phase separation shortly after the casting (Penky et al., 2003).

Macrovoid formation can be explained by several hypotheses. At some time interfacial tension between the casting solution and water bath interface becomes zero during mass transfer process. At this time water intrusion is favored which causes the initiation of fingers. Solvent from the casting solution diffuse into these intrusions causes further growth resulting in formation of macrovoids (Shojaie et al., 1994). When the difference in chemical potential of the solvent in the polymer solution and nonsolvent is lowered, then number of finger like cavities gets diminished. When the difference is large then finger like cavities is occurred (Koenhen et al., 1977).
Effective number of pores on membrane surface does not change significantly with the change of rate of evaporation. However longer evaporation time results in bigger and more uniform pores while shorter evaporation time results in smaller and less uniform pores on the membrane surface layer (Kunst and Sourirajan, 1970). Creation of higher effective number of pores is favored by higher casting solution temperature. Lower evaporation rate tends to increase productivity of films at a given level of solute separation. Number of pores, size, and distribution on the membrane surface are controlled by evaporation rate only.

Yamamura et al., (2001) has studied that at higher drying rate polymer component do not have enough time to phase separate. Hence smaller microstructure is generated at high drying rate. Matsuyama et al.(1997), has studied the effect of nonsolvent weight fraction, polymer weight fraction, and membrane thickness on membranes structures produced by dry-cast process. They found that as the nonsolvent weight fraction increases then membrane morphology changes from dense film to asymmetric to porous structure. Sambrailo and Kunst (1987) have studied that membrane performance improves with evaporation and reproducibility decreases with the evaporation. Evaporation step is not necessary in order to produce skinned membrane. Membranes with evaporation have numerous small pores hence higher product rate. Dickson et al. (1979) has studied that as the surface skin thickness increases the membrane flux decreases.

Phase inversion can be promoted by evaporating the casting solution by dry-casting process (Young et al., 2002). By controlling the drying conditions one can manipulate the membrane porosity, pore size, and permeability (Matsuyama et al., 2002). We can also produce asymmetric and symmetric membranes by controlling the polymer solution phase separation (Matsuyama et al., 2000). Final structure of membrane is determined by the rate of solvent evaporation (Young et al., 2002). Membrane morphology is greatly affected by slight change in temperature.

In the literature people have done image analysis study related to phase separating system (Altinkaya and Ozbas, 2004, Altinkaya et al, 2005 and Broens et al., 1980). In all the studied, only final microstructure has been discussed. Image is analysis is one way to study the phase separation systems. In the present work modeling and simulation study is given for the formation of asymmetric and symmetric membrane by dry-cast process. Time based study along the depth of coating will be the more rigorous analysis for phase separating systems. It will provide information about

how the microstructure is changing with time as the drying proceeds.

Various diffusion models (Alsoy and Duda, 1999, Zielinski and Hanley, 1998 and Price and Romdhane, 2003) have been developed for continuous polymer film. As the polymer-solvent-nonsolvent system phase separates, all these diffusion models may or may not be valid.

Hence, a study is needed to check the validity of various available diffusion models and time based study for phase separating systems. Cellulose acetate(3)–water(1)–acetone(2) is selected for the study because all the free volume parameters are available for this system. Water works as the nonsolvent due to low diffusion and mass transfer coefficient compared to acetone. Experimental study will performed using Confocal Raman Microscopy. It enables to catch the Raman spectra and image analysis with time within the coating. That can be convoluted to get the concentration within the coating with time.

2. Model and Simulation of Drying Coating

Fig. 1 shows the schematic of a drying coating, which has been cast on impermeable substrate. As the solvent reaches at the surface, it evaporates into the air on the top side of the coating. As mass of solvents decreasing with time, hence coating – gas interface is moving closer to the substrate opposite to diffusion. There is no mass transfer from the substrate side; hence, fluxes will be zero at the substrate.

Mass Transport:

Both the solvents are diffusing with the coating from substrate side to coating side. At anytime total mass transfer of any diffusing species is the sum of the mass transfer due to its own concentration gradient and mass transfer due to concentration gradient of second solvent.

Mass balance for solvent 1

$$\frac{\partial c_1}{\partial t} = \frac{\partial}{\partial z}\left(D_{11} \frac{\partial c_1}{\partial z} \right) + \frac{\partial}{\partial z}\left(D_{12} \frac{\partial c_2}{\partial z} \right)$$

Mass Balance for Solvent 2

$$\frac{\partial c_2}{\partial t} = \frac{\partial}{\partial z}\left(D_{21} \frac{\partial c_1}{\partial z} \right) + \frac{\partial}{\partial z}\left(D_{22} \frac{\partial c_2}{\partial z} \right)$$

The reference velocity is chosen to be volume average velocity because it is shown to be equal to zero if there is no change in volume on mixing (Cairncross, 1994).

c_i, is the concentration of solvent i, t is the time, z, is the thickness of the coatings at anytime, D_{11} and D_{22} , are main diffusion coefficients that characterize transport due to solvents own concentration gradient, D_{12} and D_{21} , are cross diffusion coefficients that characterize transport due to other solvents concentration gradient.

The concentration of polymer, balancing component, can be obtained by equating sum of mass fraction to one. Several models for predicting diffusion coefficients have been proposed in the literature. All these models are derived from Bearman's friction factor theory by making certain assumptions. Alsoy and Duda (1999) assumed that the ratio of self diffusion coefficients of solvent to polymer is equal to inverse ratio of molecular weights. Zielisnki and Hanley (1999) assumed that the ratio is equal to inverse ratio of specific volumes. Dabral et al. (2002) neglected friction between solvents when compared to friction between solvents and polymers. Price and Romdhane (2003), Nauman and Savoca (2001) reported that whenever the ratio of diffusion coefficients is a constant, the models predict negative concentration for the balancing component.

All the models are given in Table 1. D_1, and D_2 appearing in Table 1 are the self diffusion coefficients, which can be calculated using Vrentas and Duda (1977a, b) free volume theory

$$D_i = D_{0i} \exp\left(-\frac{\left(\sum_{j=1}^{N} \omega_j \hat{V}_j^* \frac{\xi_{iN}}{\xi_{jN}} \right)}{\frac{\hat{V}_{FH}}{\gamma}} \right) \quad (1)$$

$$\xi_{i3} = \frac{\textit{critical molar volume of a jumping unit of component i}}{\textit{critical molar volume of the jumping unit of the polymer}}$$

$\xi_{i3} = \dfrac{\hat{V}_i^* M_{ji}}{\hat{V}_3^* M_{j3}}$ (Vrentas et al., 1984), and

$$\frac{\hat{V}_{FH}}{\gamma} = \sum_{i=1}^{N} \frac{K_{1i}}{\gamma} \omega_i \left(K_{2i} + T - T_{gi} \right) \quad (2)$$

D_{0i}, is the pre-exponential factor for component i, ω_i , is the mass fraction of the component i, $\hat{V}_i^*$, is the specific critical hole free volume of component i required for a jump, $\hat{V}_{FH}$, is the average hole free volume per gram of mixture, γ is an overlap factor which is introduced because the same free volume is available to more than one molecule, M_{ji} , is the molecular weight of a jumping unit of component i.

Activity for the ternary polymer – solvent – solvent system can be calculated using Flory Huggins theory (Favre et al., 1996).

Table 1. Ternary Diffusion coefficients models.

Model		D_{11}	D_{12}	D_{21}	D_{22}
Alsoy and Duda	Case 1	$D_1\left[\frac{\partial \ln a_1}{\partial \ln c_1}\right]$	$\frac{c_1}{c_2}D_1\left[\frac{\partial \ln a_1}{\partial \ln c_2}\right]$	$\frac{c_2}{c_1}D_2\left[\frac{\partial \ln a_2}{\partial \ln c_1}\right]$	$D_2\left[\frac{\partial \ln a_2}{\partial \ln c_2}\right]$
	Case 2	$D_1\left[\frac{\partial \ln a_1}{\partial \ln c_1}\right]$	0	0	$D_2\left[\frac{\partial \ln a_2}{\partial \ln c_2}\right]$
	Case 3	D_1	0	0	D_2
Zielinski and Hanley		$D_1c_1\left(1-c_1\hat{V}_1+c_1\hat{V}_3\right)\left[\frac{\partial \ln a_1}{\partial c_1}\right]$ $+D_2c_1c_2\left(\hat{V}_3-\hat{V}_2\right)\left[\frac{\partial \ln a_2}{\partial c_1}\right]$	$D_1c_1\left(1-c_1\hat{V}_1+c_1\hat{V}_3\right)\left[\frac{\partial \ln a_1}{\partial c_2}\right]$ $+D_2c_1c_2\left(\hat{V}_3-\hat{V}_2\right)\left[\frac{\partial \ln a_2}{\partial c_2}\right]$	$D_2c_2\left(1-c_2\hat{V}_2+c_2\hat{V}_3\right)\left[\frac{\partial \ln a_2}{\partial c_1}\right]$ $+D_1c_1c_2\left(\hat{V}_3-\hat{V}_1\right)\left[\frac{\partial \ln a_1}{\partial c_1}\right]$	$D_2c_2\left(1-c_2\hat{V}_2+c_2\hat{V}_3\right)\left[\frac{\partial \ln a_2}{\partial c_2}\right]$ $+D_1c_1c_2\left(\hat{V}_3-\hat{V}_1\right)\left[\frac{\partial \ln a_1}{\partial c_2}\right]$

Activity coefficient of solvent 1,

$$\ln a_1 = \ln \gamma_1 + \ln \phi_1$$

$$= \ln \phi_1 + \left(1-\phi_1-\frac{\overline{V}_1}{\overline{V}_2}\phi_2\right) - \frac{\overline{V}_1}{\overline{V}_3}\phi_3 + \chi_{13}\phi_3^2 + \chi_{12}\phi_2^2 + \phi_2\phi_3\left(\chi_{13}+\chi_{12}-\frac{\overline{V}_1}{\overline{V}_2}\chi_{23}\right)$$

Activity coefficient of solvent 2,

$$\ln a_2 = \ln \gamma_2 + \ln \phi_2$$

$$= \ln \phi_2 + \left(1-\frac{\overline{V}_2}{\overline{V}_1}\phi_1-\phi_2\right) - \frac{\overline{V}_2}{\overline{V}_3}\phi_3 + \chi_{23}\phi_3^2 + \chi_{12}\frac{\overline{V}_2}{\overline{V}_1}\phi_2^2 + \phi_1\phi_3\left(\chi_{12}\frac{\overline{V}_2}{\overline{V}_1}+\chi_{23}-\frac{\overline{V}_2}{\overline{V}_1}\chi_{13}\right)$$

Where, χ, is the Flory – Huggins binary interaction parameter can be determined from the Bristow and Watson (1958) semi-empirical equation given below,

$$\chi_{ij} = 0.35 + \frac{\overline{V}_i}{RT}\left(\delta_i-\delta_j\right)^2$$

$\overline{V}_i$, is the partial molar volume of solvent i, δ_i, is the solubility parameter of solvent i, δ_j, is the solubility parameter of polymer j, and volume fraction is given by $\phi_i = c_i\hat{V}_i$,where c_i , is the concentration of species i, $\hat{V}_i$, is the specific volume of species i.

Boundary conditions at the free surface:

At the surface both the solvents are evaporating into the gas. The solvent rate of evaporation per unit area is a product of the difference in the partial pressure of the solvent at the surface of coating and in the bulk of the nearby gas and mass transfer coefficient, which is the combined action of convection and diffusion. The rate of evaporation is equal to sum of diffusive flux and convective flux at the surface of the coating. Since, volume average velocity is zero for this case. Hence, for only flux is the diffusive flux.

Flux of solvent 1 at free surface

$$\left(-D_{11}\frac{\partial c_1}{\partial z}-D_{12}\frac{\partial c_2}{\partial z}\right)\Big|_{z=L(t)} =$$

$$\left(1-c_1\overline{V}_1\right)k_1^G\left(p_{1i}^G-p_{1b}^G\right)-c_1\overline{V}_2\,k_2^G\left(p_{2i}^G-p_{2b}^G\right)$$

Flux of solvent 2 at free surface

$$\left(-D_{22}\frac{\partial c_2}{\partial z}-D_{21}\frac{\partial c_1}{\partial z}\right)\Big|_{z=L(t)} =$$

$$\left(1-c_2\overline{V}_2\right)k_2^G\left(p_{2i}^G-p_{2b}^G\right)-c_2\overline{V}_1\,k_2^G\left(p_{1i}^G-p_{1b}^G\right)$$

Boundary conditions at the base:

Since, base is impermeable. Hence, there is no mass transfer through the base to the gas.

Flux of solvent 1 at the base

$$\left(-D_{11}\frac{\partial c_1}{\partial z}-D_{12}\frac{\partial c_2}{\partial z}\right)\Big|_{z=0}=0$$

Flux of solvent 2 at the base

$$\left(-D_{22}\frac{\partial c_2}{\partial z}-D_{21}\frac{\partial c_1}{\partial z}\right)\Big|_{z=0}=0$$

Change in coating thickness:

Since both the solvents are evaporating from the surface of coating to the gas flowing parallel to the coating surface. Rate of change of mass per unit area per unit time will give the change in coating thickness.

$$\frac{dL}{dt}=-\overline{V}_1k_1^G\left(p_{1i}^G-p_{1b}^G\right)-\overline{V}_2k_2^G\left(p_{2i}^G-p_{2b}^G\right) \quad (12)$$

Where ,L is the thickness of coating, k_1^G and k_2^G, are the convective mass transfer coefficient of solvent 1 and solvent 2 respectively, $\overline{V}_1$ and $\overline{V}_2$, are the partial molar volume of solvent 1 and 2 respectively, p_{1b}^G and p_{2b}^G, are the partial pressure of solvent 1 and 2 in bulk gas respectively, p_{1i}^G, p_{2i}^G is equilibrium partial pressure of solvent 1 and solvent 2 respectively, and can be calculated by

$$p_{1i}=P_1^{vap}(T).\phi_1.\gamma_1$$

$$p_{2i}=P_2^{vap}(T).\phi_2.\gamma_2$$

γ_1 and γ_2, are the activity constants for the solvent 1 and 2 respectively.

Energy Transport

The coating is heated by hot air blown on top and bottom. Because coating is very thin, the conductive resistance of the coating is negligible compared to convective resistance in the air. Hence, the coating temperature is assumed to be uniform through the thickness (Alsoy and Duda, 1999). Detailed heat transport model of Price and Cairncross (2000) showed a temperature variation of about 0.1^0C. Temperature of coating and the substrate is assumed to be same. Radiation heat transfer is also neglected because temperatures are usually less than about 150^0C.

Heat supplied by the hot from the top side per unit area $= h^G\left(T^G-T\right)$

Heat supplied by the hot from the bottom side per unit area $= h^g\left(T^g-T\right)$

Heat taken away from the coating by the solvents vapors per unit area

$$=\sum_{i=1}^{N-1}k_{gi}^G\Delta\hat{H}_{vi}\left(p_{ii}^G-p_{ib}^G\right) \quad (10)$$

Heat accumulation within the coating per unit area = $\rho^p\hat{C}_p^pX(t)dT$ (11)

Heat accumulation within the substrate per unit area = $\rho^s\hat{C}_p^sHdT$

Heat taken by the coating + substrate = Heat supplied by the gas – Heat taken by the solvents vapors

By arranging all the terms, we will get following equation for change in coating temperature.

$$\frac{dT}{dt}=-\left[\frac{h^G\left(T-T^G\right)+\sum_{i=1}^{N-1}k_{gi}^G\Delta\hat{H}_{vi}\left(p_{ii}^G-p_{ib}^G\right)+h^g\left(T-T^g\right)}{\rho^p\hat{C}_p^pX(t)+\rho^s\hat{C}_p^sH}\right]$$

h^G and h^g, are the heat transfer coefficients at the surface of the coating and the base side respectively, $\Delta\hat{H}_{vi}$, is the enthalpy of evaporation of solvent i, ρ, is the density,

$\hat{C}_p$, is the specific heat, superscripts, p, polymer, s, substrate.

Numerical Analysis

Discretization of nonlinear ordinary and coupled differential equations (1) and (2) is done using Galerkin's finite element formulation using quadratic basis functions. Galerkin's method transforms partial differential equations into ordinary differential equations, which were integrated with ode15s of Matlab. The size of the elements increased progressively from the surface to the substrate. The position p, of i^{th} node is given by $p=\left(\frac{i-1}{n_e}\right)^2$ where i=1 to n_e+1, and n_e, is the total number of the elements. This is done to capture steep concentration gradients near the surface. Total number of nodes equal to $2n_e$+1, hence total numbers of unknown for each species are equal to $2n_e$+1, and total unknowns are $2n_e$+3 because at each time there are two other variables are temperature and the thickness of the coating. The coating was divided into 20 elements of unequal size. The time taken for the solution is around 15 to 30 min CPU time. How many elements one should will be decided based on the error analysis between two different elements. If the cumulative absolute error associated between different elements are less than or equal to 0.5%.

Generally we double the elements for the elemental analysis, 10, 20, and 40 and so on.

3. Results and Discussion

All the free volume parameters and experimental conditions for cellulose acetate (3)-water (1)-acetone(2) system are given in Table 2 and Table 3 respectively,

Table 2. Free volume parameters (Altinkaya and Ozbas, 2004)

Parameter	Unit	Cellulose Acetate / acetone	Cellulose Acetate / water
D_0	$\frac{cm^2}{s}$	3.6×10^{-4}	8.55×10^{-4}
$\frac{K_{11}}{\gamma}$	$\frac{cm^3}{g.K}$	0.000186	0.00218
$\frac{K_{12}}{\gamma}$	$\frac{cm^3}{g.K}$	0.000364	0.000364
K_{21}	K	-53.33	-152.29
K_{22}	K	-240	-240
T_{g1}	K	0	0
T_{g2}	K	0	0
$\hat{V}_1^*$	$\frac{cm^3}{g}$	0.943	1.071
$\hat{V}_2^*$	$\frac{cm^3}{g}$	1.0	1.0
ξ		0.715	0.252
χ		0.5	1.4
χ_{12}		1.3	

Effect of Nonsolvent Concentration

In the Cellulose acetate-water-acetone system, water works as the nonsolvent. From the Fig. 2, we can say that if the initial nonsolvent concentration is very low, phase separation may not take place and dense polymer film may be obtained rather than a porous membrane. At higher nonsolvent concentration the rate of shrinkage is decreased, due to lower polymer concentration the formation of more graded pore sub-layer structure having higher porosity is favored. If we further increase the water content then we will get symmetric membrane. As the water content increases the skin thickness decreases and voids volume increases. Water works as the controlling factor because of low diffusion and mass transfer coefficient. As the drying takes place the acetone evaporated faster from the top surface and surface beneath have high amount of water. Due to this initially homogenous solution becomes thermo-dynamically unstable hence phase separates.

Table 3. Experimental parameters for Cellulose acetate/water/acetone System (Altinkaya and Ozbas, 2004)

Initial Conditions	Temperature	296 K
Substrate parameters	Heat capacity	$0.75\ \frac{J}{g.K}$
	Density	$2.5\frac{cm^3}{g}$
	Base thickness	0.0508 cm
Coating parameters	Heat Capacity	$2.5\frac{J}{g.K}$
	Density of polymer	$1.31\frac{cm^3}{g}$
	Heat of evaporation of solvent 1	$2444\frac{J}{g}$
	Heat of evaporation of solvent 2	$552\frac{J}{g}$
	Bottom air supply temperature, T^g	297 K
	Top air supply temperature, T^G	297 K
	Mole fraction of the solvent 1 in the air	0
	Mole fraction of the solvent 2 in the air	0

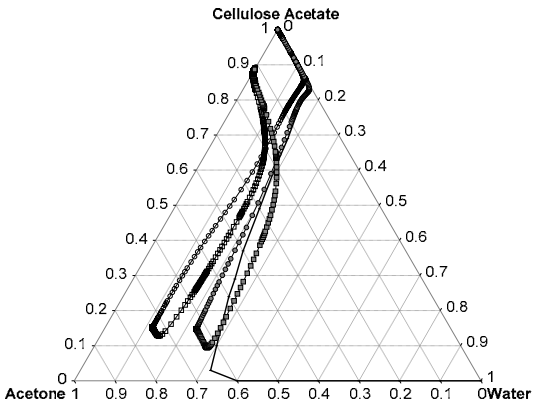

Fig.2. Concentration paths for cellulose acetate –water – acetone systems (case 1. volume fraction of cellulose acetate, water, and acetone is 10, 10 and 80

respectively, surface-air interface - ○, solution – substrate interface- □. Case.2. Volume fraction of cellulose acetate, water, and acetone is 10, 20 and 70 respectively, surface-air interface -●, solution – substrate interface- ■ , for the same thickness: 0.01cm and hear transfer coefficient: $2.2\text{x}10^{-4}\ \frac{W}{cm^2.K}$).

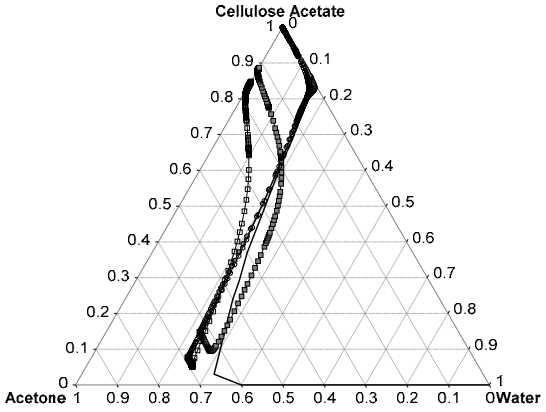

Fig. 3. Concentration paths for cellulose acetate –water-acetone system. (Case 1. volume fraction of cellulose acetate, water, and acetone is 5, 20 and 75 respectively, surface-air interface - ○, solution –substrate interface- □. Case 2. Volume fraction of cellulose acetate, water, and acetone is 10, 20 and 70 respectively, surface-air interface -●, solution –substrate interface- ■ for the same thickness: 0.01cm and hear transfer coefficient: $2.2\text{x}10^{-4}\ \frac{W}{cm^2.K}$).

Effect of Polymer Concentration

From Fig. 3, it can be concluded that at low polymer concentration we will get dense polymer film and at higher polymer concentration asymmetric polymer membrane. Since only substrate side evade the two phase region and surface side is out of two phase region. At low polymer concentration, solvent and nonslovent can diffuse easily within the film due to which skin formation does not take place. Hence no phase separation takes place. By increasing the polymer content we are increasing more resistance to solvent and non solvent diffusion hence probability to phase separation at substrate side is higher.

Effect of Coating thickness

From Fig. 4, we can say that faster phase separation is achieved by decreasing the initial film thickness due to decrease in resistance of diffusion controlled mass transfer. It favors less asymmetric membranes because top and bottom polymer concentrations are same. As the thickness increases, then delay in phase transition is expected due to increase in the total mass of acetone. It causes greater asymmetry in final structure with thicker densified layer near free surface.

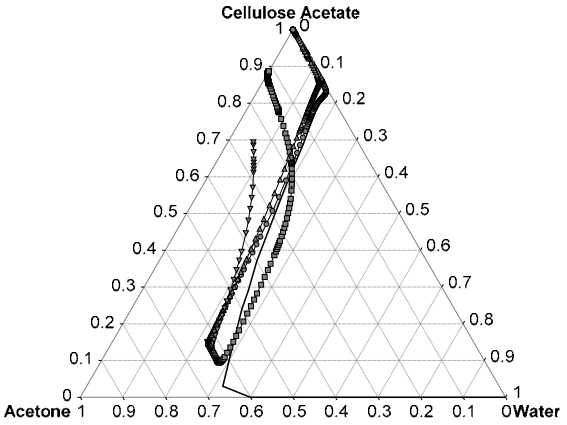

Fig.4. Concentration paths for cellulose acetate –water-acetone system. (Case 1. thickness: 0.01cm, surface-air interface-●, solution–substrate interface- ■. Case.2. Thickness: 0.05cm, surface-air interface-▲, solution–substrate interface-▼. For the same volume fraction of cellulose acetate, water and acetone is 10, 20 and 70 respectively and hear transfer coefficient: $2.2\text{x}10^{-4}\ \frac{W}{cm^2.K}$).

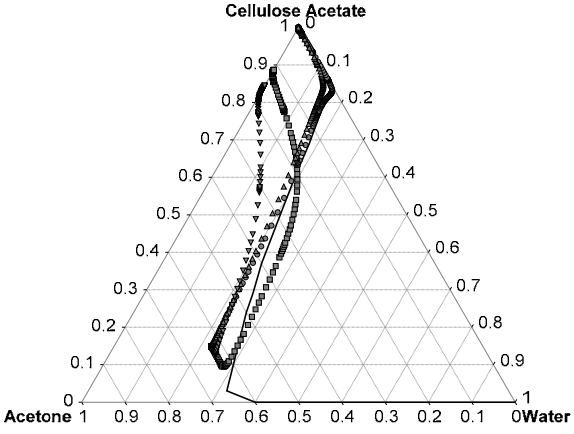

Fig.5. Concentration paths for cellulose acetate –water-acetone system (Case 1. heat transfer coefficient: $2.2\text{x}10^{-4}\frac{W}{cm^2.K}$, surface-air interface-●, solution – substrate interface- ■. Case 2. Heat transfer coefficient: $8.4\text{x}10^{-4}\ \frac{W}{cm^2.K}$, surface-air interface-▲, solution – substrate interface-▼. For the same volume fraction of cellulose acetate, water and acetone is 10, 20 and 70 respectively and thickness: 0.01cm).

Effect of Air Velocity

From Fig. 5, we can say that as we increase the air velocity the phase separation is completely suppressed and uniformly dense coating devoid of substantial microstructure will result.

At higher air flow rate of evaporation will be higher than the diffusion mass transfer. Top surface becomes dried very soon however beneath we have much amount of water and acetone which favor the phase separation. Hence, we are likely to get the asymmetric membranes. At low air flow rate external mass transfer is less compared to diffusion controlled mass transfer rate. Drying takes place slowly and have high acetone content. Higher amount of acetone favor homogeneous polymer film.

4. Conclusion

Based on the simulation results we can conclude the following;

1. We can produce asymmetric and symmetric membrane by dry casting method by changing the drying conditions.
2. Low water content give dense polymer film however high water content gives asymmetric and then symmetric membranes without changing the polymer content.
3. Above certain amount of polymer we will get membrane for the same amount of water.
4. Phase separation totally is suppressed at high air velocity.

Acknowledgements

This work was funded by King Abdul Aziz City for Science and Technology (KACST) (Grant Number: 79-25).

References

1. Alsoy, S. and Duda, J.L., 1999, "Modeling of Multicomponent Drying of Polymer Films", AICHE Journal, 45, 4, 896-905.
2. Altinkaya, Sacide Alsoy and Ozbas, Bulent, 2004, "Modeling of asymmetric membrane formation by dry – casting method", Journal of Membrane Science, 230, 71–89.
3. Altinkaya, Sacide Alsoy, Yenal, Hacer and Ozbas, Bulent, 2005, "Membrane Formation by dry-cast process model validation through morphological studies", Journal of Membrane Science, 249, 163 – 172.
4. Broens, L., Altena, F.W. Smolders, C.A. and Koenhen, D.M., 1980, "Asymmetric Membrane Structures as a Result of phase separation phenomena", Desalination, 32, 33 – 45.
5. Dickson, J.M., Lloyd, D.R. and Huang, R.Y.M., 1979, "Ionically crosslinked Poly (acrylic acid) Membranes. III. Reverse Osmosis Results for Dry Cast Membranes" Journal of Applied Polymer Science, 24, 1341 – 1351.
6. Koenhen, D. M., Mulder, M.H.V. and Smolders, C.A., 1977, "Phase separation Phenomena during the Formation of Asymmetric Membranes", Journal of Applied Polymer Science, 21, 199-215.
7. Krantz, W.B., Ray, R.J., Sani, R.L. and Gleason, K.J., 1986, "Theoretical Study of the Transport Processes Occurring During the Evaporation Step in Asymmetric Membrane Casting", 29, 11 – 36.
8. Kunst, B. and Sourirajan, S., 1970, "Effect of Casting Conditions on the Performance of Porous Cellulose Acetate Membranes in Reverse Osmosis", Journal of Applied Polymer Science, 14, 723-733.
9. Matsuyama, H., Kim, M. and Lloyd, D. R., 2002, "Effect of extraction and drying on the structure of microporous polyethylene membranes prepared via thermally induced phase separation", Journal of Membrane Science, 2004, 413-419.
10. Matsuyama, H., Nishiguchi, M. and Kitamura, Y., 2000, "Phase Separation Mechanism during Membrane Formation by Dry-Cast Process", Journal of Applied Polymer Science, 77, 776-782.
11. Matsuyama, H., Teramoto, M. and Uesaka, T., 1997, "Membrane Formation and Structure Development by dry-cast Process", Journal of Membrane Science, 135, 271-288.
12. Penky, M.R., Zartman, J., Krantz, W.B., Greenberg, A.R. and Todd, P., 2003, "Flow-Visualization during macrovoids pore formation in dry-cast cellulose acetate membranes", Journal of Membrane Science, 211, 71-90.
13. Price, P.E. and Romdhane, I.H., 2003, "Multicomponent Diffusion Theory and Its Application to Polymer-Solvent Systems", AICHE Journal, 49, 2, 309-322.
14. Sambrailo, D. and Kunst, B., 1987, "Asymmetric Membrane Formation. Is the Evaporation Step Necessary?" Desalination, 64, 321-328.
15. Shojaie, S. S., Krantz, W. B. and Greenberg, A. R., 1994, "Dense Polymer Film and Membrane Formation via the dry-cast process Part II. Model

validation and morphological studies", Journal of Membrane Science, 94, 281 – 298.

16. Shojaie, Saeed S., Krantz, William B. and Greenberg, Alan R., 1994, "Dense polymer film and membrane formation via the dry-cast process Part I.Model development", Journal of Membrane Science, 94, 255 – 280.
17. Yamamura, M., Nishio, T., Kajiwara, T. and Adachi, K., 2001, "Effect of stepwise change of drying rate on microstructure evolution in polymer films", Drying Technology, 19, 7, 1397-1410.
18. Young, T.H., Huang, J.H. and Chuang, W.Y., 2002, "Effect of evaporation temperature on the formation of particulate membranes from crystalline polymers by dry-cast process", European Polymer Journal, 38, 63-72.
19. Zielinski, J.M. and Hanley, B., 1999, "Practical Friction-Based Approach to Modeling Multicomponent Diffusion", AICHE